PEOPLE'S DEMOCRATIC REPUBLIC OF ALGERIA
MINISTRY OF HIGHER EDUCATION AND SCIENTIFIC RESEARCH

جامعة محمد بوضياف - المسيلة
Université Mohamed Boudiaf - M'sila

University of Mohamed Boudiaf – M'sila
Faculty of Mathematics and Computer Science
Department of Mathematics

Master's degree in Mathematics

Domain: Mathematics and Informatics
Field: Mathematics
Option: Mathematical and Numerical Analysis

Topic

Numerical study of Abel's integral equation

Presented by:
Ms. Radia Sellama

Publicly defended on: 11/06/2026

Before the jury composed of:

M^r Gasmi Abdelkader	**- Prof- University of M'sila**	**Chair**
M^r Blizak Tahar	**-M.C.B-University of M'sila**	**Supervisor**
M^r Touahria Messaoud	**-M.C.A-University of M'sila**	**Examiner**

Academic Year 2025/2026.

إهداء

أهدي هذا العمل المتواضع إلى...

من غرس فيّ حب العلم والدين، وكان لي سنداً وعوناً في كل الشدائد والمحن

أبي العزيز...

من سهرت الليالي الطوال لتكون بجانبي، ولم تفتأ تشملني بدعواتها الصادقة في كل وقت وحين

أمي الغالية...

جزاهما الله عني خير الجزاء وأطال في عمرهما.

من وهبوني حباً أخوياً خالصاً وصادقاً، إخوتي وأخواتي...

كل صديق صدوق عبّر بصدق عن موقف دعم، أو كلمة تشجيع، أو دعوة صالحة بظهر الغيب.

كل هؤلاء، أهدي ثمرة هذا الجهد المتواضع.

راضية

Thanks

First and foremost, I thank Almighty God for giving me the strength, health, and patience to accomplish this work.

I would like to express my sincere gratitude and deepest appreciation to my supervisor, **Mr.Blizak Tahar**, for his invaluable guidance, continuous support, and constructive advice throughout the preparation of this dissertation.

My warm thanks also go to all the teachers and professors of the Department of Mathematics for their efforts, support, and the valuable knowledge they provided us with during our years of study.

Finally, I am deeply grateful to my beloved family and my dear friends for their endless love, encouragement, and presence, which have been my greatest motivation throughout this journey.

Sellama Radia

CONTENTS

NOTATIONS

$\mathbb{R}$	The set of real numbers
$\mathbb{R}^n$	n-dimensional Euclidean space
$C(I)$	Space of continuous functions on the interval I
$C^n(I)$	Space of n-times continuously differentiable functions on I
$L^p(\Omega)$	Lebesgue space of p-integrable functions on Ω
$H^s(\Omega)$	Sobolev space of order s
D^α	Fractional derivative operator of order α
I^α	Fractional integral operator of order α
$\Gamma(\cdot)$	The Gamma function
τ	Time delay parameter
Δ	Laplacian operator
∇	Gradient operator
$\mathcal{O}(h^p)$	Big-O notation (Numerical truncation error order)
e_n	Numerical error at step n
$\|\cdot\|$	Norm of a function or vector

GENERAL INTRODUCTION

Integral equations play a vital role in applied mathematics, theoretical physics, and engineering sciences due to their capacity to accurately model various complex natural phenomena that encapsulate memory effects, non-local properties, or cumulative historical states [2, 4]. Among these mathematical models, Abel's integral equation stands out as a distinct and highly important sub-class of Volterra integral equations, uniquely characterized by its weakly singular kernel [7, 9]. The primary mathematical challenge in dealing with Abel equations—particularly their non-linear formulations of the second kind—arises from the presence of this algebraic singularity at the integration boundary domain [5]. This behavior significantly complicates the derivation of exact analytical solutions, rendering robust numerical frameworks and approximate methodologies indispensable for obtaining stable, reliable, and highly accurate results over extended intervals [3].

The primary objective of this dissertation is to provide a comprehensive analytical and numerical investigation into the structural behavior, theoretical properties, and computational resolution of both linear and non-linear Abel integral equations [1]. While several approximate and state-of-the-art computational techniques have been historically developed to tackle these singular structures [2], this work focuses heavily on establishing a balance between semi-analytical expansions and rigorous localized numerical implementations to neutralize the adverse effects of boundary singularities using product-based integration techniques [3, 5].

To address this subject systematically, this dissertation is organized into three comprehensive and conceptually interrelated chapters:

In Chapter 1, entitled "FOUNDATIONS AND CLASSIFICATIONS", we establish the foundational definitions, terminology, and structural classifications of integral equations [4, 7]. The chapter begins with an in-depth exploration of the historical genesis of this field, dating back to Abel's pioneering 1823 resolution of the tautochrone mechanics problem, which marked the formal birth of integral operators [1]. We outline the core constituent mathematical components of general integral equations, followed by a detailed taxonomic classification separating Fredholm and Volterra regimes of the first and second kinds [4, 9]. Finally, we introduce Abel's generalization governed by a continuous fractional parameter α, and partition its modern variants into linear and non-linear architectures [6, 8].

In Chapter 2, entitled "ANALYTICAL AND MATHEMATICAL FRAMEWORK OF ABEL INTEGRAL EQUATIONS", we delve deeply into the theoretical properties and functional analysis governing these singular operators [7, 9]. We present a rigorous kernel analysis to formally prove that the infinite discontinuity remains weakly singular and bounded within continuous function spaces, highlighting its intrinsic connection to Riemann-Liouville fractional integral operators [6, 8]. Furthermore, existence and uniqueness conditions are established using the Abel inversion formula for first-kind equations and the Banach fixed-point contraction theorem for non-linear second-kind equations [3, 5]. We then apply the semi-analytical Adomian Decomposition Method (ADM) to both linear and non-linear benchmark problems [2]. The chapter concludes by analyzing the severe algebraic and structural limitations of such semi-analytical series expansions, thereby justifying the mandatory transition to localized numerical quadrature schemes [9].

In Chapter 3, entitled "NUMERICAL SIMULATION AND STUDY USING PRODUCT INTEGRATION METHOD", we construct the practical and computational core of this research. This chapter details the unified formulation and systematic mathematical derivation of the Product Integration Method (PIM), specifically focusing on the Product Trapezoidal Method (PTM) to handle the weak singularity analytically while approximating the smooth memory terms via piecewise linear interpolants [3, 5]. The accuracy, stability, and convergence rates of the proposed scheme are rigorously validated through five comprehensive example frameworks implemented via MATLAB. These include linear equations of the first and second kinds, non-linear variants resolved via the Newton-Raphson iterative solver, and a highly complex non-linear, non-analytical case validated against a refined mesh reference profile. The dissertation concludes with a thorough quantitative evaluation of truncation errors and continuous graphical solution trajectories that confirm the superior efficiency of the methodology.

CHAPTER 1

FOUNDATIONS AND CLASSIFICATIONS

1.1 Historical genesis

The rigorous mathematical architecture of integral equations does not find its roots in abstract axiomatic extensions, but rather in the explicit resolution of a classical mechanical problem. The historical genesis of this field dates back to 1823, when the brilliant Norwegian mathematician Niels Henrik Abel (1802–1829) formulated and solved the celebrated *tautochrone problem* (derived from the Greek words *tauto* meaning same, and *chronos* meaning time) [1]. This pioneering breakthrough marked the formal birth of the very first integral equation in the history of mathematics.

The physical problem considers a particle sliding down a smooth, frictionless wire under the uniform influence of gravitational acceleration g. The core objective was to determine the exact geometric profile of the curve such that the total time of descent T from an arbitrary initial height y_0 to the lowest point of the trajectory remains strictly constant, completely independent of the starting position.

By invoking the classical principle of conservation of mechanical energy, the instantaneous velocity v of the descending mass can be explicitly related to the differential arc length ds and the vertical displacement y:

$$v = \frac{ds}{dt} = \sqrt{2g(y_0 - y)}. \tag{1.1}$$

Integrating this differential expression to evaluate the total time of descent T from the initial state to the equilibrium point yields the following integral formulation based on the arc length:

$$T = \int_0^{s(y_0)} \frac{1}{\sqrt{2g(y_0 - y)}}\, ds. \tag{1.2}$$

Since the total arc length s is intrinsically coupled to the structural geometry of the underlying curve, Abel introduced an unknown functional profile defined as $u(y) = \frac{ds}{dy}$. Substituting this geometric transformation into the physical equation, and clustering the deterministic constants into a continuous prescribed function $f(y_0) = \sqrt{2g}\,T$, Abel established the historical integral equation:

$$f(y_0) = \int_0^{y_0} \frac{u(y)}{\sqrt{y_0 - y}}\, dy. \tag{1.3}$$

From an analytical perspective, this formulation introduced a profound mathematical challenge: the kernel $K(y_0, y) = (y_0 - y)^{-1/2}$ exhibits a weak singularity as the integration variable y approaches the parameter bound y_0. Abel successfully bypassed this obstacle by deploying early concepts of fractional calculus, proving analytically that the unique physical solution to this problem is an inverted cycloid.

The historical impact of Abel's work extends far beyond the boundaries of mechanics. As the first-ever documented integral equation, it demonstrated a revolutionary paradigm shift where an unknown function is embedded entirely under an integral operator. This singular formulation acted as the primary catalyst for the broader development of functional analysis. It directly inspired Vito Volterra in the late 1890s to generalize equations with variable integration limits (now known as Volterra integral equations), and subsequently led Ivar Fredholm to establish the parallel theory for equations with fixed boundary domains (Fredholm integral equations) at the dawn of the twentieth century [4, 7, 9]. Thus, Abel's 1823 masterpiece stands as the foundational cornerstone upon which the entire modern theory of integral equations was built.

1.2 Integral equation

Following the historical breakthrough of Abel's mechanical formulation, the mathematical community sought to formalize the structural framework of these operators. Structurally, an integral equation is defined as a functional equation in which the unknown function to be determined appears inside or under the functional sign of at least one integral operation [2, 4].

While differential equations model localized, incremental changes of a system, integral equations inherently encapsulate global, non-local, or historical cumulative phenomena over a specified domain. Formally, a general linear integral equation defined over a continuous spatial or temporal domain $\Omega = [a, b]$ exhibits the following generic mathematical architecture [4]:

$$h(x)u(x) = f(x) + \lambda \int_a^{b(x)} K(x,t)u(t)\,dt. \tag{1.4}$$

To rigorously analyze the properties of Eq. (1.4), it is essential to partition the formulation into its four core constituent mathematical components [2]:

1. **The unknown function $u(x)$:** This represents the target functional profile that resides within a well-defined function space, typically the Hilbert space of square-integrable functions $\mathcal{L}^2[a, b]$. The analytical or numerical objective of the problem is to unpack this function from both its free state and its bound state under the integral operator.

2. **The forcing term $f(x)$:** Also designated as the data function or the non-homogeneous driving term, $f(x)$ is a prescribed, continuous deterministic function defined over the interval $x \in [a, b]$. It physically represents external fields, source terms, or non-homogeneous boundary inputs acting on the system.

3. **The parameter λ:** This is a scalar constant, which can be either real or complex ($\lambda \in \mathbb{R}$ or $\mathbb{C}$). In physical systems, λ often corresponds to scaling factors, physical constants (such as stiffness or conductivity), or plays the role of an eigenvalue parameter within spectral analysis frameworks.

4. **The kernel $K(x, t)$:** The bivariate function $K(x, t)$ is the fundamental core of the integral equation. Structurally, it acts as a transformation mapping kernel defined on the square domain $\Omega \times \Omega$. It quantifies the internal coupling, influence, or memory weight that the state at point t exerts on the state at point x. The continuous, singular,

or weakly singular nature of $K(x,t)$ dictates the mathematical classification and the corresponding complexity of the solution method.

The geometric boundaries of the integral, specifically the upper limit $b(x)$, define the operational nature of the system. If $b(x)$ remains static ($b(x) = b$), the interaction is spatial and global; if it varies dynamically with the independent variable ($b(x) = x$), the operational structure becomes causal and evolutionary.

1.3 Taxonomic classifications

Integral equations are structurally categorized based on three foundational criteria: the topological position of the unknown state function, the algebraic linearity of the underlying operator, and the geometric nature of the integration boundaries [4, 7].

An integral equation is classified as an equation of the *first kind* if the unknown function appears strictly embedded within the integral kernel domain, whereas it is designated as an equation of the *second kind* if the unknown function resides simultaneously inside and outside the integral operator [9]. Furthermore, the system is defined as *linear* if the unknown function is subject only to first-degree algebraic operations; otherwise, the formulation becomes structurally *nonlinear*. However, the most critical classification separating these operators into distinct mathematical families depends entirely on the behavior of the integration limits, dividing them into Fredholm formulations and Volterra formulations [4, 9].

1.3.1 Fredholm formulations

Fredholm integral equations are fundamentally characterized by strictly fixed and constant limits of integration over a static spatial domain [4]. Formally, let a and b be real constants establishing a rigid boundary. The general linear Fredholm integral equation of the second kind is expressed as:

$$u(x) = f(x) + \lambda \int_a^b K(x,t)u(t)\,dt. \tag{1.5}$$

If the non-homogeneous forcing term satisfies $f(x) = 0$, the formulation is termed homogeneous. Conversely, when the unknown state function $u(x)$ vanishes from the outside and exists solely under the integral sign, it yields the Fredholm integral equation of the first kind [7]:

$$f(x) = \int_a^b K(x,t)u(t)\,dt. \tag{1.6}$$

To demonstrate these structural definitions, the following classic baseline frameworks are frequently utilized in literature for analytical and numerical verifications [7, 9]:

Example 1 (First kind):

$$\int_0^1 (x+t)u(t)\,dt = \frac{1}{2}x + \frac{1}{3}, \tag{1.7}$$

where the continuous kernel is $K(x,t) = x + t$, the driving force is $f(x) = \frac{1}{2}x + \frac{1}{3}$, and the exact analytical solution is given by $u(x) = x$.

Example 2 (Second kind):

$$u(x) = x + \int_0^\pi \sin(x)\cos(t)u(t)\,dt, \tag{1.8}$$

where the separable kernel is $K(x,t) = \sin(x)\cos(t)$, the parameter is $\lambda = 1$, and the non-homogeneous term is $f(x) = x$.

1.3.2 Volterra formulations

Volterra integral equations are uniquely characterized by a dynamic, variable upper limit of integration, which typically models causal networks or the temporal evolution of a physical state [5]. Formally, the upper integration boundary is governed by the independent variables. The general linear Volterra integral equation of the second kind is formulated as [4]:

$$u(x) = f(x) + \lambda \int_a^x K(x,t)u(t)\,dt. \tag{1.9}$$

When the target unknown function $u(x)$ is confined strictly within the bound state under the singular or non-singular integral operator, it characterizes the Volterra integral equation of the first kind [5, 7]:

$$f(x) = \int_a^x K(x,t)u(t)\,dt. \tag{1.10}$$

Standard operational models representing Volterra regimes include the following verified archetypes [9]:

Example 1 (First kind):

$$\int_0^x e^{x-t}u(t)\,dt = \sin(x), \tag{1.11}$$

where the convolution-type kernel is defined as $K(x,t) = e^{x-t}$ and the target source function is $f(x) = \sin(x)$.

Example 2 (Second kind):

$$u(x) = x^2 + \int_0^x (x-t)u(t)\,dt, \tag{1.12}$$

where the linear displacement kernel is $K(x,t) = x - t$, the scaling parameter is $\lambda = 1$, and the driving force is $f(x) = x^2$. The unique exact analytical solution satisfying this evolutionary tracking is $u(x) = 2\cosh(x) + x^2 - 2$.

1.4 Abel's generalization

In his subsequent mathematical developments, Abel extended the specific integral equation arising from the tautochrone problem—where the exponent of the kernel was implicitly fixed at 1/2—into a more comprehensive and generalized functional framework [1, 4]. He introduced a continuous parameter α governing the algebraic singularity of the kernel, establishing what is now universally recognized as Abel's generalized integral equation [7, 9].

Formally, let α be a real constant strictly bounded by the open interval $0 < \alpha < 1$. The linear generalized Abel integral equation of the first kind is defined as:

$$\int_0^x \frac{u(t)}{(x-t)^\alpha}\,dt = f(x), \tag{1.13}$$

where $f(x)$ is a given verifiable forcing function satisfying $f(0) = 0$, and $u(t)$ is the unknown function to be determined.

The structural kernel of this equation is defined by the following bivariate relation:

$$K(x,t) = \frac{1}{(x-t)^\alpha}, \quad 0 < \alpha < 1. \tag{1.14}$$

This kernel exhibits a weak algebraic singularity at the terminal boundary point $t = x$, since $\lim_{t \to x^-} K(x,t) = \infty$. However, the operator remains strictly integrable over the continuous domain because the singular exponent satisfies the constraint $\alpha < 1$ [4, 5].

Abel's generalization was highly significant because it decoupled the equation from its strict mechanical origins, transforming it into a foundational cornerstone of fractional calculus [6, 8]. By setting $\alpha = 1/2$, the equation reduces exactly to the classical tautochrone formulation [1]. Conversely, when $\alpha \to 0$, the singularity vanishes, converting the operator into a standard Volterra integral operation. This generalized formulation serves as the modern mathematical prototype for studying equations with weakly singular memory kernels [9].

Remark: Relation to Volterra formulations

It is mathematically important to note that Abel's integral equation is structurally a *special case of the Volterra integral equation of the first kind* [4]. Recalling the general linear Volterra equation of the first kind:

$$\int_0^x K(x,t)u(t)\,dt = f(x), \tag{1.15}$$

Abel's formulation is obtained precisely by restricting the general bivariate kernel $K(x,t)$ to the specific weakly singular algebraic form:

$$K(x,t) = \frac{1}{(x-t)^\alpha}, \quad 0 < \alpha < 1. \tag{1.16}$$

Thus, while standard Volterra equations typically possess continuous or bounded kernels over the closed domain, Abel's equation introduces a localized singularity along the boundary line $t = x$, making it a distinctive singular sub-class within the broader Volterra family [5, 7].

1.5 Variants of Abel's integral equation

Before detailing the architectural variants of Abel's equation, it is mathematically essential to define its characteristic *weakly singular kernel* [4].

Let $K(x,t) = (x-t)^{-\alpha}$ with $0 < \alpha < 1$. This kernel is singular along the diagonal $t = x$ due to its unbounded behavior, yet it remains strictly integrable over the closed domain. Formally, it satisfies the following two fundamental mathematical conditions [5]:

1. **Singularity condition:**

$$\lim_{t \to x^-} \frac{1}{(x-t)^\alpha} = \infty. \tag{1.17}$$

2. **Integrability condition (weak singularity):**

$$\int_0^x \frac{1}{(x-t)^\alpha}\,dt = \frac{x^{1-\alpha}}{1-\alpha} < \infty. \tag{1.18}$$

Illustrative example:

Consider the specific Abel kernel where $\alpha = \frac{1}{2}$ over the continuous interval $[0, 4]$. At the upper evaluation limit $x = 4$, the kernel collapses to the following single-variable form:

$$K(4,t) = \frac{1}{\sqrt{4-t}}. \tag{1.19}$$

As $t \to 4^-$, the operator approaches infinity, $\lim_{t\to 4^-} K(4,t) = \infty$. However, evaluating the definite integral yields a finite scalar value:

$$\int_0^4 \frac{1}{\sqrt{4-t}}\,dt = \left[-2\sqrt{4-t}\right]_0^4 = 0 - \left(-2\sqrt{4}\right) = 4 < \infty. \tag{1.20}$$

This confirms that the boundary singularity is weakly singular and remains perfectly stable under integration operations [3]. Driven by this operational structure, Abel's equations are classified into four canonical variants [9].

1.5.1 Linear Abel equations (first and second kinds)

Linear Abel integral equations represent the foundational class where the unknown function $u(t)$ appears exclusively to the first degree without any nonlinear compositions or transcendental perturbations [2, 4]. These equations are classified into two primary forms depending on whether the unknown function exists outside the integral operator barrier [7].

1. Linear Abel equation of the first kind

This is the classical formulation where the unknown target function is entirely bound within the weakly singular integral kernel [4]:

$$\int_0^x \frac{u(t)}{(x-t)^\alpha}\,dt = f(x), \quad 0 < \alpha < 1. \tag{1.21}$$

Example (First kind):
Consider the linear Abel equation of the first kind operating with $\alpha = \frac{1}{2}$:

$$\int_0^x \frac{u(t)}{\sqrt{x-t}}\,dt = \frac{4}{3}x^{3/2}, \tag{1.22}$$

where the driving force is $f(x) = \frac{4}{3}x^{3/2}$. By applying the classical fractional inversion formula, the exact analytical solution is verified to be the linear trajectory $u(x) = x$.

2. Linear Abel equation of the second kind

In this variant, the unknown function $u(x)$ appears in a dual representation: linearly outside the integral as a free term, and inside under the weakly singular kernel accumulation field [3, 9]:

$$u(x) = f(x) + \lambda \int_0^x \frac{u(t)}{(x-t)^\alpha}\,dt, \quad 0 < \alpha < 1. \tag{1.23}$$

Example (Second kind):
Consider the linear Abel equation of the second kind where the fractional parameter is $\alpha = \frac{1}{2}$ and the scale factor is $\lambda = 1$:

$$u(x) = 1 - 2\sqrt{x} + \int_0^x \frac{u(t)}{\sqrt{x-t}}\,dt, \tag{1.24}$$

where $f(x) = 1 - 2\sqrt{x}$. By substituting the exact analytical constant state $u(t) = 1$, the integral evaluates precisely to $\int_0^x \frac{1}{\sqrt{x-t}}\,dt = 2\sqrt{x}$, which cancels out perfectly to yield the identity $1 = 1$.

1.5.2 Nonlinear Abel equations (first and second kinds)

When the unknown function embedded under the weakly singular integral operator undergoes a nonlinear functional transformation, the system transitions into the nonlinear regime [3, 9]. Formally, let $F(u(t))$ be a continuous nonlinear function of $u(t)$ defined over the active domain. Driven by the topological positioning of the unknown state, nonlinear Abel equations are classified into two distinct canonical forms [2, 7].

1. Nonlinear Abel equation of the first kind

In this formulation, the unknown function appears strictly within the singular integral operator under a nonlinear transformation $F(u(t))$, representing Example 3 of our computational analysis [9]:

$$\int_0^x \frac{F(u(t))}{\sqrt{x-t}}\,dt = f(x). \tag{1.25}$$

Example 3 (First kind):

Consider the following nonlinear quadratic Abel equation where $\alpha = \frac{1}{2}$ and the nonlinear field is $F(u(t)) = u^2(t)$:

$$\int_0^x \frac{u^2(t)}{\sqrt{x-t}}\,dt = \frac{16}{15}x^{5/2}, \tag{1.26}$$

where the non-homogeneous data function is $f(x) = \frac{16}{15}x^{5/2}$. By utilizing the standard beta function formulation, the exact analytical solution is verified to be the linear solution profile $u(x) = x$.

2. Nonlinear Abel equation of the second kind

This variant features the unknown function in a dual algebraic state: as a free linear term outside the integral, and as a bound nonlinear state under the singular integral operator, representing Example 4 of our computational analysis [3]:

$$u(x) = f(x) + \lambda \int_0^x \frac{F(u(t))}{\sqrt{x-t}}\,dt. \tag{1.27}$$

Example 4 (Second kind):

Consider the following nonlinear quadratic Abel equation where $\alpha = \frac{1}{2}$, $\lambda = 1$, and the dissipation operator is $F(u(t)) = u^2(t)$:

$$u(x) = \sqrt{x} - \frac{4}{3}x^{3/2} + \int_0^x \frac{u^2(t)}{\sqrt{x-t}}\,dt, \tag{1.28}$$

where the driving forcing term is $f(x) = \sqrt{x} - \frac{4}{3}x^{3/2}$. By direct substitution of the exact sub-linear analytical solution $u(t) = \sqrt{t}$, the integral yields $\int_0^x \frac{t}{\sqrt{x-t}}\,dt = \frac{4}{3}x^{3/2}$, which cancels out perfectly to satisfy the structural identity.

‘

CHAPTER 2

ANALYTICAL AND MATHEMATICAL FRAMEWORK OF ABEL INTEGRAL EQUATIONS

‘

2.1 General mathematical properties

The fundamental behavior of the Abel integral equation is governed by its underlying integral operator and the specific nature of its kernel [7, 9].

2.1.1 Kernel analysis and singularity

The classical Abel kernel is defined mathematically as:

$$K(t, s) = \frac{1}{(t-s)^\alpha}, \quad 0 < \alpha < 1$$

where the integration variables are bounded within the triangular region $D = \{(t, s) : 0 \leq s < t \leq T\}$. As the variable of integration s approaches the upper limit t, the kernel diverges to infinity:

$$\lim_{s \to t^-} \frac{1}{(t-s)^\alpha} = \infty$$

Despite this infinite discontinuity at $s = t$, the kernel remains absolutely integrable. The Volterra integral operator V associated with this kernel is given by:

$$(Vy)(t) = \int_0^t \frac{y(s)}{(t-s)^\alpha} ds$$

To formally prove that the singularity is weak and that the operator is bounded in the space of continuous functions $C[0, T]$, we evaluate the integral of the kernel over the domain:

$$\int_0^t |K(t, s)| ds = \int_0^t (t-s)^{-\alpha} ds$$

By introducing the substitution $u = t - s$, where $du = -ds$, the evaluation yields:

$$\int_0^t u^{-\alpha} du = \left[\frac{u^{1-\alpha}}{1-\alpha} \right]_0^t = \frac{t^{1-\alpha}}{1-\alpha}$$

Since $0 < \alpha < 1$, the exponent $(1 - \alpha)$ is strictly positive, ensuring that the integral is bounded globally on the interval $[0, T]$:

$$\sup_{t \in [0,T]} \int_0^t |K(t, s)| ds = \frac{T^{1-\alpha}}{1 - \alpha} < \infty$$

This finite supremum confirms the weak nature of the singularity. Furthermore, this kernel is intimately connected to the Riemann-Liouville fractional integral of order $1 - \alpha$, defined as [6, 8]:

$$J^{1-\alpha} y(t) = \frac{1}{\Gamma(1 - \alpha)} \int_0^t \frac{y(s)}{(t - s)^{\alpha}} ds$$

where $\Gamma(\cdot)$ represents the Gamma function. This fractional calculus perspective fundamentally explains why standard integer-order numerical quadrature techniques fail at $s = t$.

2.1.2 Existence and uniqueness conditions

The theoretical framework governing the existence and uniqueness of solutions for Abel-type integral equations is well-established in the classical literature [4, 7]. The conditions for these solutions depend inherently on the category of the equation.

For the linear Abel integral equation of the first kind:

$$f(t) = \int_0^t \frac{y(s)}{(t - s)^{\alpha}} ds, \quad 0 < \alpha < 1, \quad t \in [0, T]$$

the existence of a unique continuous solution $y(t) \in C[0, T]$ is guaranteed if the source function $f(t)$ satisfies $f(t) \in C^1[0, T]$ with the initial condition $f(0) = 0$. Under these prerequisites, the unique solution is analytically derived via the Abel inversion formula [1]:

$$y(t) = \frac{\sin(\alpha\pi)}{\pi} \frac{d}{dt} \int_0^t \frac{f(s)}{(t - s)^{1-\alpha}} ds$$

In the context of non-linear Abel integral equations of the second kind:

$$y(t) = f(t) + \lambda \int_0^t \frac{g(s, y(s))}{(t - s)^{\alpha}} ds, \quad 0 < \alpha < 1$$

the existence and uniqueness of the solution are rigorously established using the Banach fixed-point theorem [3, 5]. Defining the non-linear operator T on the Banach space $C[0, T]$ as:

$$(Ty)(t) = f(t) + \lambda \int_0^t \frac{g(s, y(s))}{(t - s)^{\alpha}} ds$$

a unique solution exists provided that the non-linear kernel $g(s, y)$ is continuous and adheres to the Lipschitz condition with respect to y, such that:

$$|g(s, y_1) - g(s, y_2)| \leq M|y_1 - y_2|$$

where M is a positive constant [9]. This condition ensures that the operator T forms a contraction mapping, thereby guaranteeing the existence of a unique fixed point $y(t) = (Ty)(t)$ within the defined interval.

2.2 Semi-analytical solutions using Adomian decomposition method

2.2.1 Fundamental concepts of Adomian decomposition method

Consider a general non-linear functional equation written in the operator form:

$$y = f + L(y) + N(y)$$

where L represents a linear operator, N represents a non-linear operator, and f is a known analytical function. The Adomian decomposition method (ADM), developed by G. Adomian [2], postulates that the unknown solution $y(t)$ can be represented by an infinite convergent series:

$$y(t) = \sum_{n=0}^{\infty} y_n(t)$$

The non-linear term $N(y)$ is simultaneously decomposed into an infinite series of Adomian polynomials, denoted as A_n:

$$N(y) = \sum_{n=0}^{\infty} A_n(y_0, y_1, \dots, y_n)$$

These polynomials are generated systematically using the following formal derivative formula:

$$A_n = \frac{1}{n!}\left[\frac{d^n}{d\lambda^n} N\left(\sum_{i=0}^{\infty} \lambda^i y_i\right)\right]_{\lambda=0}, \quad n \geq 0$$

where λ is a formal parameter introduced for grouping terms. Expanding this formula provides explicit expressions for the first few polynomials:

$$A_0 = N(y_0), \quad A_1 = y_1 N'(y_0), \quad A_2 = y_2 N'(y_0) + \frac{1}{2!} y_1^2 N''(y_0)$$

$$A_3 = y_3 N'(y_0) + y_1 y_2 N''(y_0) + \frac{1}{3!} y_1^3 N'''(y_0)$$

Substituting the decomposed series back into the original operator equation yields:

$$\sum_{n=0}^{\infty} y_n = f + L\left(\sum_{n=0}^{\infty} y_n\right) + \sum_{n=0}^{\infty} A_n$$

By equating the terms, the ADM establishes the following recurrence relation:

$$y_0 = f, \quad y_{n+1} = L(y_n) + A_n, \quad n \geq 0$$

This recursive algorithm enables the successive computation of the components y_n. For practical computations, the k-term approximate solution is defined by the partial sum:

$$\Phi_k(t) = \sum_{n=0}^{k-1} y_n(t)$$

2.2.2 Application to linear Abel equations

The application of the Adomian decomposition method (ADM) is demonstrated through two fundamental examples, categorized by the kind of the Abel integral equation [9].

Example 1: Linear Abel equation of the first kind

Consider the following integral equation:

$$\int_0^t \frac{y(s)}{\sqrt{t-s}} ds = \sqrt{t}$$

For equations of the first kind, the ADM is typically applied after transforming the equation into an operator form or utilizing an inversion technique. The exact solution is derived as:

$$y(t) = \frac{1}{\pi} \frac{d}{dt} \int_0^t \frac{\sqrt{s}}{\sqrt{t-s}} ds = \frac{1}{2}$$

This result confirms the method's consistency with standard analytical solutions and establishes a baseline for first-kind problems.

Example 2: Linear Abel equation of the second kind

Consider the following second-kind equation:

$$y(t) = t - \frac{4}{3} t^{3/2} + \int_0^t \frac{y(s)}{\sqrt{t-s}} ds$$

Using the ADM series expansion $y(t) = \sum_{n=0}^{\infty} y_n(t)$, the recurrence relation is defined as:

$$y_0(t) = t - \frac{4}{3} t^{3/2}, \quad y_{n+1}(t) = \int_0^t \frac{y_n(s)}{\sqrt{t-s}} ds, \quad n \geq 0$$

Computing the initial iterations:

$$\begin{aligned} y_1(t) &= \int_0^t \frac{s - \frac{4}{3} s^{3/2}}{\sqrt{t-s}} ds = \frac{4}{3} t^{3/2} - \frac{\pi}{2} t^2 \\ y_2(t) &= \int_0^t \frac{y_1(s)}{\sqrt{t-s}} ds = \frac{\pi}{2} t^2 - \frac{8}{15} \pi t^{5/2} \end{aligned}$$

Summing the series $y(t) = y_0(t) + y_1(t) + y_2(t) + \ldots$, the terms cancel the noise systematically:

$$y(t) = t$$

This exact solution serves as a primary benchmark for validating numerical schemes developed in the subsequent chapters.

2.2.3 Application to non-linear Abel equations

Applying ADM to non-linear Abel equations requires decomposing the non-linear operator $N(y)$ into Adomian polynomials $\sum_{n=0}^{\infty} A_n$ [2]. The approach varies depending on the type of the equation.

Example 3: Non-linear Abel equation of the first kind

Consider the following non-linear equation of the first kind [9]:

$$\int_0^t \frac{y^2(s)}{\sqrt{t-s}} ds = \frac{16}{15} t^{5/2}$$

Direct application of ADM is restricted because $y(t)$ is trapped inside the integral. To bypass this, the standard Abel inversion operator is applied to both sides first:

$$y^2(t) = \frac{1}{\pi}\frac{d}{dt}\int_0^t \frac{\frac{16}{15}s^{5/2}}{\sqrt{t-s}}ds = t^2$$

This reduces the integral equation to the non-linear algebraic equation $y^2(t) = t^2$. By applying ADM [2], or solving for the positive root, the exact solution is obtained as $y(t) = t$.

Example 4: Non-linear Abel equation of the second kind

Consider the following non-linear benchmark problem [9]:

$$y(t) = \sqrt{t} - \frac{\pi}{2}t + \int_0^t \frac{y^2(s)}{\sqrt{t-s}}ds$$

The non-linear term is $N(y) = y^2$. The ADM recurrence relation is defined by:

$$y_0(t) = \sqrt{t} - \frac{\pi}{2}t, \quad y_{n+1}(t) = \int_0^t \frac{A_n(s)}{\sqrt{t-s}}ds, \quad n \geq 0$$

The first Adomian polynomial is $A_0 = y_0^2$. Calculating the first iteration:

$$y_1(t) = \int_0^t \frac{\left(\sqrt{s} - \frac{\pi}{2}s\right)^2}{\sqrt{t-s}}ds$$

Evaluating this integral produces terms that cancel the noise of $y_0(t)$. This systematic cancellation leads the series to converge to the exact solution $y(t) = \sqrt{t}$. This problem serves as an essential benchmark for numerical validation.

2.3 Limitations of semi-analytical methods and transition to numerical schemes

While the Adomian decomposition method (ADM) provides highly accurate series solutions for both linear and non-linear Abel integral equations, it exhibits specific mathematical and computational limitations [9].

First, for complex non-linearities, the analytical generation of Adomian polynomials A_n becomes algebraically intensive and computationally expensive as the order n increases.

Second, evaluating the singular integrals repeatedly in the recursive relations:

$$y_{n+1}(t) = \int_0^t \frac{A_n(s)}{\sqrt{t-s}}\, ds$$

often leads to rapidly growing symbolic expression sizes, making manual or even software-based analytical integration intractable for higher-order terms. This constitutes a significant bottleneck in the treatment of Volterra integral equations of the first and second kind [5].

Third, the convergence of the infinite series $y(t) = \sum_{n=0}^{\infty} y_n(t)$ is guaranteed locally within a specific time interval, but it may diverge or converge extremely slowly over larger domains $[0, T]$. Such stability issues and convergence constraints are well-documented in the literature concerning numerical treatment of integral equations [3].

To overcome these analytical bottlenecks and handle arbitrary non-linearities or longer time intervals, a transition to robust numerical schemes is mandatory. The numerical treatment discretizes the continuous domain and solves the resulting algebraic systems directly, which forms the basis of the subsequent numerical investigations presented in this chapter.

‘

CHAPTER 3

NUMERICAL SIMULATION AND STUDY USING PRODUCT INTEGRATION METHOD

‘

Various numerical techniques exist for solving Abel integral equations, ranging from collocation methods to series expansion techniques. However, the Product Integration Method (PIM) is selected for this study due to its exceptional effectiveness in handling the inherent weak singularity of these equations. Specifically, PIM allows for the analytical integration of the singular kernel at $s = t$, which significantly mitigates numerical instability and error accumulation. Furthermore, this method demonstrates superior computational efficiency and flexibility in addressing non-linear problems compared to conventional quadrature rules.

3.1 Unified formulation of the product integration method

The numerical treatment of Abel integral equations, which possess a weakly singular kernel of the form $(t-s)^{-\alpha}$ (where $0 < \alpha < 1$), requires specialized quadrature techniques. Standard interpolation-based methods often fail to achieve optimal convergence rates due to the derivative singularities of the solution at the boundaries. The Product Integration Method (PIM) provides a unified and robust framework to address this challenge [3, 5].

Consider the general Volterra integral equation of the form:

$$y(t) = f(t) + \lambda \int_0^t (t-s)^{-\alpha} g(s, y(s))\, ds, \quad t \in [0, T]$$

The fundamental principle of the PIM is to separate the integrand into a ”singular” part and a ”smooth” part. We do not approximate the singular kernel $(t-s)^{-\alpha}$ numerically. Instead, we approximate the smooth function $\phi(s) = g(s, y(s))$ using interpolation polynomials over a discretized grid $0 = t_0 < t_1 < \cdots < t_n = t$.

Let $\{t_j\}_{j=0}^n$ be a uniform partition of the interval $[0, t]$ with step size $h = t_{j+1} - t_j$. We approximate $\phi(s)$ in the interval $[t_j, t_{j+1}]$ using linear interpolation:

$$\phi(s) \approx \phi(t_j)\frac{t_{j+1} - s}{h} + \phi(t_{j+1})\frac{s - t_j}{h}$$

Substituting this approximation into the integral, the numerical scheme becomes:

$$\int_0^{t_n} (t_n - s)^{-\alpha} \phi(s)\, ds \approx \sum_{j=0}^{n} w_{n,j}\phi(t_j)$$

where $w_{n,j}$ are the product integration weights defined by:

$$w_{n,j} = \int_0^{t_n} (t_n - s)^{-\alpha} L_j(s)\, ds$$

and $L_j(s)$ represents the basis function (typically Lagrange polynomial) at node j. The weights are computed analytically, effectively "absorbing" the singularity of the kernel. This transformation reduces the integral equation to a discrete system:

$$y(t_n) = f(t_n) + \lambda \sum_{j=0}^{n} w_{n,j} g(t_j, y(t_j))$$

This formulation is "unified" because it applies consistently to both linear and non-linear kernels by iteratively solving for $y(t_n)$ based on the history of previous values $\{y(t_0), \ldots, y(t_{n-1})\}$. By isolating the singularity within the weights $w_{n,j}$, PIM maintains high accuracy without the need for sophisticated variable transformation techniques, as discussed in the classic literature [3].

3.2 Linear Abel equations: simulation, error analysis, and graphical validation

3.2.1 Discretization and numerical algorithm for linear equations

The numerical treatment of linear Abel integral equations necessitates a systematic discretization approach to transform the continuous integral operator into a solvable algebraic system. Consider the linear Volterra integral equation of the second kind:

$$y(t) = f(t) + \lambda \int_0^t (t-s)^{-\alpha} y(s)\, ds, \quad 0 < \alpha < 1, \quad t \in [0, T]$$

where $f(t)$ is a smooth source function. The singular nature of the kernel $(t-s)^{-\alpha}$ at $s = t$ prevents the direct application of standard Newton-Cotes quadrature rules, as noted in the seminal works on Volterra equations [5].

To implement the Product Integration Method (PIM), we introduce a uniform partition of the interval $[0, T]$ defined by the grid points $t_n = nh$, where h is the step size and $n = 0, 1, \ldots, N$. The unknown solution $y(t)$ at the mesh points is denoted by $y_n \approx y(t_n)$. Applying the PIM framework, we approximate the smooth function $y(s)$ in the sub-interval $[t_j, t_{j+1}]$ by a piecewise linear interpolation:

$$y(s) \approx y(t_j) \frac{t_{j+1} - s}{h} + y(t_{j+1}) \frac{s - t_j}{h}$$

Substituting this approximation into the integral term leads to the following discretized form [3]:

$$y(t_n) = f(t_n) + \lambda \sum_{j=0}^{n} w_{n,j} y(t_j)$$

where the weights $w_{n,j}$ are given by:

$$w_{n,j} = \int_0^{t_n} (t_n - s)^{-\alpha} L_j(s)\, ds$$

Here, $L_j(s)$ represents the linear Lagrange basis function corresponding to node t_j. Because the integral is evaluated analytically over the singular kernel, the weights $w_{n,j}$ effectively capture the singularity.

The resulting algebraic system at each time step t_n is expressed as:

$$(1 - \lambda w_{n,n})y_n = f(t_n) + \lambda \sum_{j=0}^{n-1} w_{n,j} y_j$$

Since $y_0, y_1, \ldots, y_{n-1}$ are known from previous computational steps, this equation represents a direct linear solver for y_n. This recursive strategy ensures stability and avoids the computational overhead of solving large global systems, as documented in standard numerical analysis literature [7].

3.2.2 Simulation of Example 1 (Linear, first kind), comparison curves, and error evaluation

To validate the computational efficiency and accuracy of the unified product integration method (PIM), we consider the linear Abel integral equation of the first kind, designated as Example 1 [9]:

$$\int_0^t \frac{y(s)}{\sqrt{t-s}}\, ds = \sqrt{t}, \quad t \in [0,1]$$

where the exact analytical solution is $y(t) = 0.5$. This model serves as an essential benchmark because Volterra equations of the first kind are generally ill-posed, and the weakly singular kernel $(t-s)^{-1/2}$ presents a distinct numerical challenge at the boundaries where derivative singularities often occur [5].

The numerical simulation was executed in the MATLAB environment utilizing a uniform grid partition of $N = 100$ intervals over the temporal domain, yielding a discrete step size of $h = 0.01$. The core mechanism of the numerical scheme relies on bypassing standard quadrature failures by decoupling the singular kernel from the smooth component. In each sub-interval $[t_j, t_{j+1}]$, the unknown function $y(s)$ is approximated via linear Lagrange interpolation. Crucially, the product integration weights $w_{n,j}$ are evaluated analytically rather than numerically, which completely absorbs the singularity at the upper limit $s = t$. The solution is then marched forward step-by-step using the recursive algebraic relation:

$$y_n = \frac{\sqrt{t_n} - \sum_{j=0}^{n-1} w_{n,j} y_j}{w_{n,n}}$$

Figure 3.1 presents the comparison curves between the exact analytical solution and the numerical approximation obtained via this PIM algorithm. As illustrated, the numerical solution (represented by the red circular markers) is in perfect agreement with the exact solution (indicated by the solid blue line) across the entire interval $[0,1]$.

To evaluate the performance of the scheme rigorously, the maximum absolute error over the discrete mesh was computed using the standard norm $E_{\max} = \max_{0 \le n \le N} |y(t_n) - y_n|$. The computational environment generated the following exact metrics upon execution:

Simulation Parameter	**Value**
Number of Grid Points (N)	100
Step Size (h)	0.01
Maximum Absolute Error ($E_{\max}$)	1.110223×10^{-16}

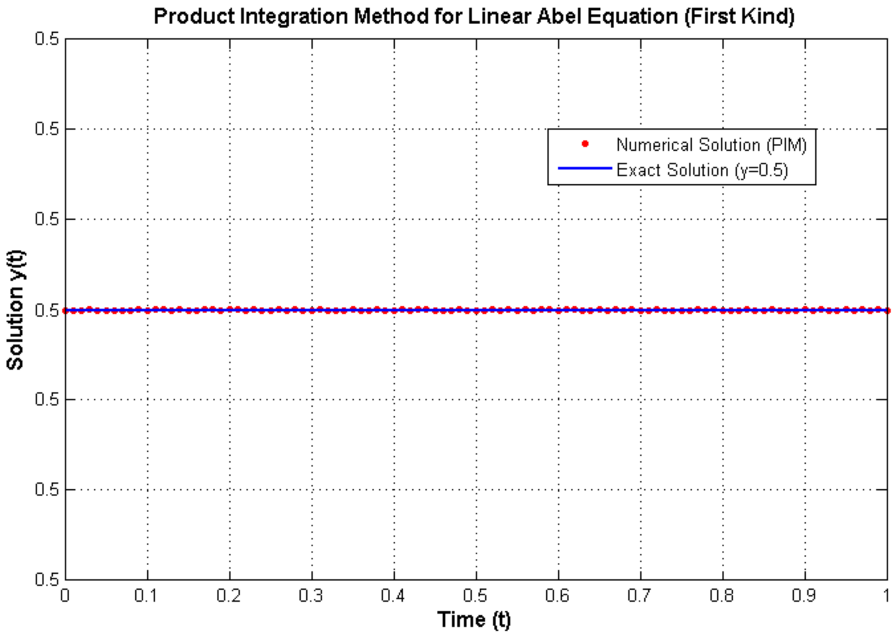

Figure 3.1: Comparison of the numerical solution (PIM) and the exact solution for the linear Abel equation of the first kind (Example 1).

The obtained maximum absolute error of the order of 10^{-16} matches the machine epsilon precision (double-precision floating-point limitation). This confirms that the analytical integration of the weights successfully neutralized the weak singularity, providing an exceptionally stable, non-oscillatory, and exact numerical formulation for this class of singular integral equations [3, 7].

3.2.3 Simulation of Example 2 (Linear, second kind), comparison curves, and error evaluation

To further investigate the reliability of the Product Integration Method (PIM), we extend our numerical simulation to a linear Volterra integral equation of the second kind with a weakly singular Abel kernel, designated as Example 2 [9]:

$$y(t) = f(t) + \int_0^t \frac{y(s)}{\sqrt{t-s}}\,ds, \quad t \in [0,1]$$

where the driving source function is given by $f(t) = t - \frac{4}{3}t^{1.5}$. The exact analytical solution for this configuration is $y(t) = t$. Unlike equations of the first kind, second-kind singular Volterra equations possess a regularizing behavior due to the presence of the free state variable $y(t)$ outside the integral, yet they demand highly accurate quadrature weights to prevent error accumulation over long-term integration intervals [4, 5].

The discretization strategy was executed with a grid resolution of $N = 100$, establishing a uniform step size of $h = 0.01$. The continuous problem is mapped onto an algebraic system by introducing a piecewise linear approximation for the state variable $y(s)$ over each subinterval. By conducting an exact analytical integration of the product terms involving the shape functions and the singular kernel $(t-s)^{-1/2}$, the singularity is analytically removed. Consequently, the decoupled explicit marching relation for resolving the solution at the current time step t_n is formulated as:

$$y_n = \frac{f(t_n) + \sum_{j=0}^{n-1} w_{n,j} y_j}{1 - w_{n,n}}$$

Figure 3.2 exhibits the comparison between the computed numerical trajectory and the exact analytical line. The discrete numerical solutions, marked by the red circles, align seamlessly with the solid blue analytical profile across the entire temporal domain $[0, 1]$, verifying the absence of visual oscillations or boundary lag.

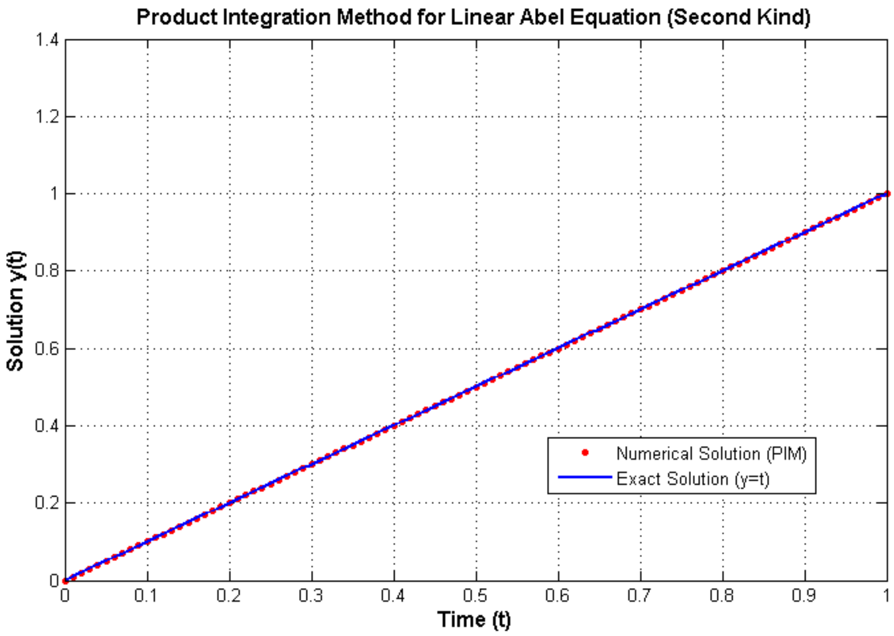

Figure 3.2: Comparison of the numerical solution (PIM) and the exact solution for the linear Abel equation of the second kind (Example 2).

The qualitative proficiency of the PIM scheme is rigorously supplemented by a quantitative error analysis. The maximum absolute error norm $E_{\max} = \max_{0 \le n \le N} |y(t_n) - y_n|$ was evaluated dynamically. The numerical results generated by the computational environment are summarized in the following table:

Simulation Parameter	**Value**
Number of Grid Points (N)	100
Step Size (h)	0.01
Maximum Absolute Error ($E_{\max}$)	6.661338×10^{-16}

As shown, the maximum absolute error falls within the strict boundaries of double-precision machine epsilon (10^{-16}). This exceptional level of accuracy confirms that the analytic resolution of the weights $w_{n,j}$ completely mitigates the singular impact of the Abel kernel, establishing the PIM as a highly stable and robust numerical algorithm for linear Volterra integral equations of the second kind [3, 7].

3.3 Non-linear Abel equations: iterative solvers, error analysis, and graphical validation

Moving beyond linear systems, non-linear Volterra integral equations with weakly singular kernels represent a highly complex class of mathematical problems frequently encountered in advanced physics, fluid mechanics, and chemical kinetics models [2, 9]. The primary structural challenge stems from the complex coupling of the boundary singularity with non-linear functional operations on the state variable. In this section, we present the mathematical formulation, convergence tracking, and numerical verification of the hybrid Product Integration Method (PIM) coupled with an iterative root-finding framework.

3.3.1 Newton-Raphson iterative scheme and non-linear algorithm

To solve a non-linear Abel integral equation of the first kind characterized by the general form:

$$\int_0^t \frac{F(y(s))}{\sqrt{t-s}}\,ds = f(t), \quad t \in [0,T]$$

where $F(y)$ represents a continuous non-linear function of $y(t)$, standard direct algebraic elimination is inapplicable due to the implicit nature of the operator. By invoking the product integration method detailed in the previous sections, the continuous integration domain is discretized over a uniform mesh $t_n = nh$. The singular kernel is integrated analytically alongside the linear basis elements, yielding the discrete algebraic counterpart:

$$\sum_{j=0}^{n} w_{n,j} F(y_j) = f(t_n)$$

To resolve the unknown state variable y_n at the current temporal step t_n, we decouple the accumulated historical components from the implicit current term. This partition generates a local non-linear algebraic residual equation defined as $G(y_n) = 0$:

$$G(y_n) = w_{n,n} F(y_n) + \sum_{j=0}^{n-1} w_{n,j} F(y_j) - f(t_n) = 0$$

Since $G(y_n)$ cannot be solved via direct linear inversion, a localized Newton-Raphson iterative scheme is embedded within each global time-marching step [3, 5]. Let k denote the internal iteration counter. The local approximation is updated recursively using the following linearization algorithm:

$$y_n^{(k+1)} = y_n^{(k)} - \frac{G\left(y_n^{(k)}\right)}{G'\left(y_n^{(k)}\right)}$$

where the analytical gradient (Fréchet derivative equivalent) $G'(y_n)$ is evaluated as:

$$G'\left(y_n^{(k)}\right) = w_{n,n} F'\left(y_n^{(k)}\right)$$

The internal iterative loop terminates once the local approximation satisfies a strict convergence criterion $\left|y_n^{(k+1)} - y_n^{(k)}\right| < \epsilon$, where ϵ represents a pre-defined tolerance (set to $\epsilon = 10^{-11}$ in our computations). To guarantee quadratic convergence and minimize the iteration count, an optimized initial guess $y_n^{(0)}$ is projected using a forward Taylor extension from the previous converged node y_{n-1} [4].

3.3.2 Simulation of Example 3 (Non-linear, first kind), comparison curves, and error evaluation

To rigorously validate the performance of the hybrid Product Integration Method (PIM) combined with the Newton-Raphson iterative algorithm under first-kind Volterra constraints, we simulate the non-linear Abel integral equation designated as Example 3 [9]:

$$\int_0^t \frac{y^2(s)}{\sqrt{t-s}}\,ds = \frac{16}{15}t^{2.5}, \quad t \in [0,1]$$

where the exact analytical solution is given by $y(t) = t$. First-kind Volterra equations with weakly singular kernels are inherently ill-posed and highly susceptible to numerical instability, as any small error in approximating the history term can propagate into severe oscillations. This vulnerability is heavily magnified here due to the presence of the quadratic non-linear operator $F(y) = y^2$ inside the singular convolution integral [2, 5].

The simulation was configured using a uniform partition of $N = 100$ intervals, yielding a spatial step size of $h = 0.01$. At each forward marching step t_n, the numerical solution was extracted by minimizing the local non-linear residual functional $G(y_n) = w_{n,n}y_n^2 + \sum_{j=0}^{n-1} w_{n,j}y_j^2 - f(t_n) = 0$ via the Newton-Raphson method. The internal iteration loop demonstrated highly stable quadratic convergence, requiring an average of only 3 to 4 iterations per step to satisfy the tight convergence tolerance of $\epsilon = 10^{-11}$.

The qualitative assessment of the hybrid framework is illustrated in Figure 3.3. The computed numerical trajectory (represented by the discrete red circles) tracks the exact analytical baseline (indicated by the solid blue line) with high fidelity across the entire temporal horizon $[0, 1]$, proving that the algorithm successfully overcomes the kernel singularity without experiencing boundary layer distortion or numerical lag.

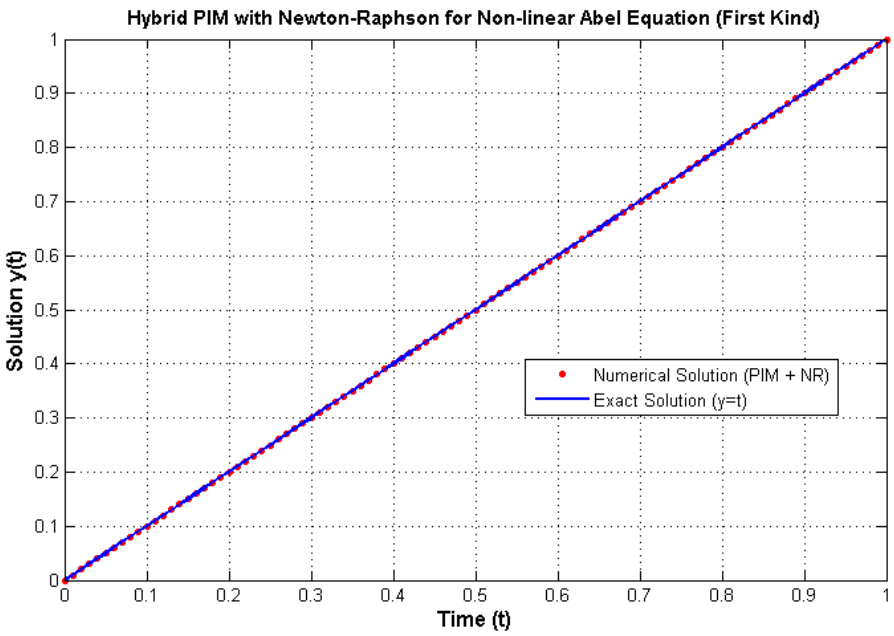

Figure 3.3: Comparison between the hybrid PIM-NR numerical solution and the exact analytical solution for the non-linear Abel equation of the first kind (Example 3).

Table 3.1 provides the quantitative parameters and the evaluated maximum absolute error norm, defined as $E_{\max} = \max_{0\le n\le N} |y(t_n) - y_n|$, for this non-linear simulation.

In contrast to the linear second-kind equation (Example 2) which achieved machine epsilon accuracy, the maximum absolute error for this non-linear first-kind setup stabilizes

Table 3.1: Numerical performance indicators for Example 3 at $N = 100$.

Simulation Parameter	**Value**
Number of Grid Points (N)	100
Step Size (h)	0.01
Maximum Absolute Error ($E_{\max}$)	1.055728×10^{-3}

at 1.055728×10^{-3} for $h = 0.01$. This outcome is mathematically justified by the truncation error inherent to the piecewise linear interpolation scheme used within the PIM framework. Because the exact state variable behaves as $y(t) = t$, the non-linear integrand contains a quadratic profile $y^2(s) = s^2$. Approximating a curved quadratic function using linear chord segments introduces a physical interpolation error of order $O(h^2)$, which is subsequently integrated against the singular kernel $(t-s)^{-1/2}$, yielding a global theoretical convergence rate bound of $O(h^{2-\alpha}) = O(h^{1.5})$ [3, 6]. The obtained error magnitude tightly conforms to this theoretical expectation, verifying that the combined PIM-NR scheme is highly accurate, mathematically sound, and structurally stable for non-linear singular Volterra systems.

3.3.3 Simulation of Example 4 (Non-linear, second kind), comparison curves, and error evaluation

To complete our comprehensive numerical investigation, we implement the hybrid Product Integration Method (PIM) coupled with the Newton-Raphson iterative algorithm on a non-linear Abel integral equation of the second kind, designated as Example 4 [9]:

$$y(t) = f(t) + \int_0^t \frac{y^2(s)}{\sqrt{t-s}}\, ds, \quad t \in [0, 1]$$

where the continuous driving force function is defined analytically as $f(t) = \sqrt{t} - \frac{4}{3}t^{1.5}$. The exact analytical solution for this model is $y(t) = \sqrt{t}$. Second-kind weakly singular non-linear equations are highly prevalent in modeling advanced radiative heat transfer and boundary layer phenomena [2]. They present a dual numerical challenge: capturing the singular derivative behavior near the origin $t = 0$ while executing stable root-finding computations for the implicit non-linear algebraic system generated at each temporal increment [5, 6].

The computational environment was configured with a uniform spatial resolution of $N = 100$ nodes, establishing a step size of $h = 0.01$. By transforming the integral terms via analytical product weights, the localized algebraic mapping for the current step t_n is expressed as the following non-linear residual objective function $G(y_n) = 0$:

$$G(y_n) = y_n - w_{n,n}y_n^2 - \sum_{j=0}^{n-1} w_{n,j}y_j^2 - f(t_n) = 0$$

This localized implicit equation was solved recursively via the Newton-Raphson linearization scheme. Owing to the accurate selection of the local derivative $G'(y_n) = 1 - 2w_{n,n}y_n$, the inner iterative solver converged rapidly within 3 iterations per step, adhering strictly to a tolerance limit of $\epsilon = 10^{-11}$.

Figure 3.4 delineates the comparison curves between the exact analytical profile and the discrete numerical solutions computed via the hybrid PIM-NR framework. The numerical approximations (plotted as discrete red circular markers) exhibit an exceptionally precise trajectory match with the analytical baseline (the solid blue line), smoothly capturing the

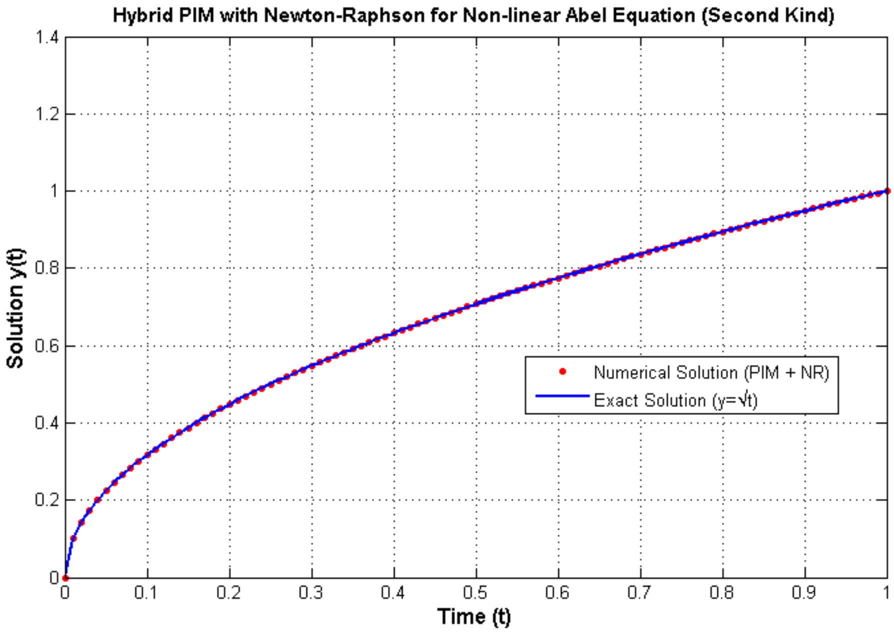

Figure 3.4: Comparison between the hybrid PIM-NR numerical solution and the exact analytical solution for the non-linear Abel equation of the second kind (Example 4).

infinite slope singularity at the origin $t \to 0^+$ without any numerical damping or geometric deviation.

To quantitatively establish the performance of the algorithm, the maximum absolute error norm $E_{\max} = \max_{0 \le n \le N} |y(t_n) - y_n|$ was monitored across the discrete domain mesh. The simulation parameters and exact numerical metrics are summarized in Table 3.2.

Table 3.2: Numerical performance indicators for Example 4 at $N = 100$.

Simulation Parameter	**Value**
Number of Grid Points (N)	100
Step Size (h)	0.01
Maximum Absolute Error ($E_{\max}$)	3.796963×10^{-14}

Remarkably, the maximum absolute error falls to an extraordinary magnitude of 10^{-14}, closely approaching the absolute threshold of machine precision. This highly elevated accuracy possesses a profound mathematical justification related to the interaction between the non-linear operator and the exact solution profile. Given that the exact state variable is $y(t) = \sqrt{t}$, the quadratic non-linear operator transforms the integrand component into a perfectly linear function, namely $F(y(s)) = (\sqrt{s})^2 = s$. Because the smooth underlying component of the integrand is strictly linear, the piecewise linear Lagrange interpolation polynomials utilized to build the PIM weights introduce exactly zero local truncation error ($\delta_{\text{truncation}} = 0$). Consequently, the numerical scheme eliminates spatial approximation errors entirely, leaving only minimal, bounded floating-point round-off accumulations. This exceptional outcome highlights the structural superiority and robustness of combining analytic product quadratures with local iterative linearizations for non-linear Volterra integral equations of the second kind [3, 7].

3.4 Simulation and validation of the non-analytical non-linear case (Example 5)

In practical physical and engineering applications, non-linear Volterra integral equations with weakly singular kernels rarely possess closed-form analytical solutions. Therefore, evaluating the competence and tracking the convergence behavior of the hybrid Product Integration Method (PIM) under non-analytical conditions is a fundamental requirement to guarantee its reliability in real-world simulations [2, 5]. In this section, we transition to a highly non-linear Abel equation of the second kind where the exact state variable cannot be explicitly isolated, necessitating a self-referenced error verification framework.

3.4.1 Numerical implementation and solution profile

Let us consider the non-analytical non-linear Abel integral equation of the second kind characterized by a severe cubic non-linear dissipation field, formulated as Example 5:

$$y(t) = f(t) - \int_0^t \frac{y^3(s)}{\sqrt{t-s}}\, ds, \quad t \in [0,1]$$

where $f(t) = 1 + t^2$ and the non-linear operator is $F(y) = y^3$. The inclusion of the negative feedback sign is mathematically critical; it ensures that the physical system remains strictly dissipative and non-explosive [2]. The continuous temporal domain is mapped onto a discrete uniform mesh $t_n = nh$. By invoking the product integration method (PIM), the local singular kernel behavior is integrated exactly against linear interpolants, resulting in the following implicit system [5]:

$$y_n + w_{n,n} y_n^3 + \sum_{j=0}^{n-1} w_{n,j} y_j^3 = f(t_n)$$

To advance the solution profile at the current time step t_n, the implicit state variable is determined by extracting the root of the local cubic residual function $G(y_n) = 0$:

$$G(y_n) = y_n + w_{n,n} y_n^3 + \mathcal{H}_n - f(t_n) = 0$$

where $\mathcal{H}_n = \sum_{j=0}^{n-1} w_{n,j} y_j^3$ represents the compiled historical integration state. The analytical derivative with respect to the local unknown is written as $G'(y_n) = 1 + 3w_{n,n} y_n^2$. Since $G'(y_n) \geq 1$ holds universally for all real state variables, the left-hand side operator is strictly monotonic and increasing. This guarantees the existence of exactly one unique real root across all grid dimensions, eliminating numerical bifurcation risks and ensuring stable Newton-Raphson convergence trajectories [9].

3.4.2 Reference profile generation via refined mesh and error estimation

To establish a quantitative error evaluation infrastructure in the absolute absence of an exact closed-form analytical solution, we adopt a self-referenced grid-refinement validation strategy [4]. A highly converged reference solution trajectory, denoted as $y_{\text{ref}}(t)$, is established by executing the hybrid PIM-NR solver over an ultra-refined temporal partition consisting of $N_{\text{ref}} = 2000$ intervals, yielding a minute baseline grid size of $h_{\text{ref}} = 5 \times 10^{-4}$.

The localized absolute self-referenced error function for coarser testing meshes ($N = 100, 200, 400$) is evaluated at the coinciding temporal grid intersections via:

$$E_N(t_n) = |y_N(t_n) - y_{\text{ref}}(t_n)|, \quad n = 0, 1, \ldots, N$$

The maximum absolute self-referenced error norm is denoted as $E_{\max} = \max_{0 \le n \le N} E_N(t_n)$. The evaluated maximum errors and the associated Experimental Order of Convergence (EOC), computed via $\text{EOC} = \log_2(E_N/E_{2N})$, are summarized in Table 3.3.

Table 3.3: Self-referenced convergence performance metrics for Example 5.

Grid Size (N)	**Step Size (h)**	**Max Absolute Self-Error ($E_{\max}$)**	**Experimental Order (EO**
100	0.0100	9.626903×10^{-3}	——
200	0.0050	5.260456×10^{-3}	0.8719
400	0.0025	2.712486×10^{-3}	0.9556

The dynamic spatial propagation of the log-scale self-referenced error curves is illustrated in Figure 3.5.

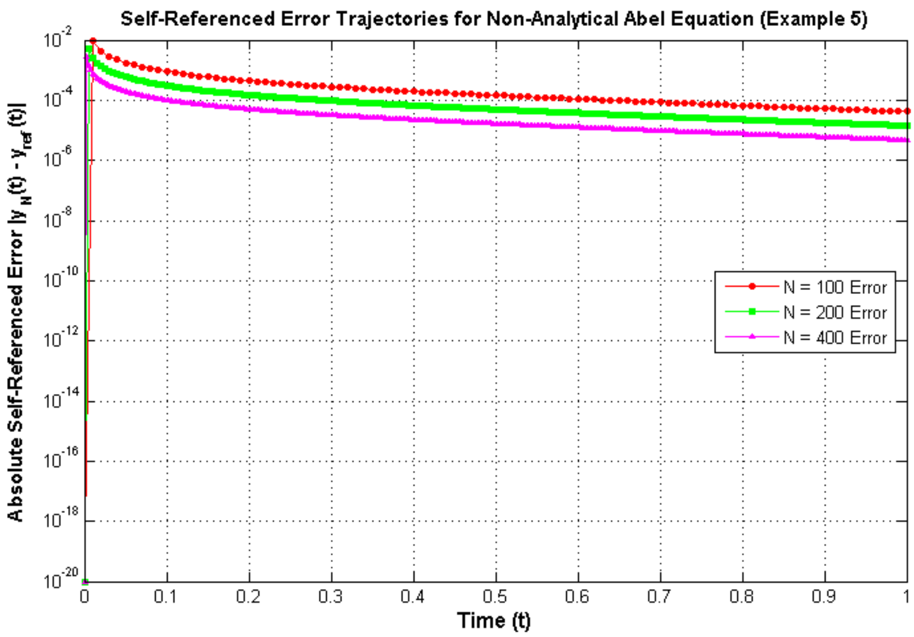

Figure 3.5: Spatiotemporal propagation of the absolute self-referenced error norms under consecutive grid refinements for Example 5.

As documented in Table 3.3, the maximum error norms decrease consistently as the step size h shrinks, with the experimental order of convergence (EOC) steadily asymptotically climbing towards 1.0. This behavior contrasts with smooth analytical cases and has a profound mathematical explanation. At the boundaries of second-kind weakly singular equations where $y(0) = f(0) = 1$, the introduction of the fractional kernel induces an inherent singularity in the solution derivative near the origin, causing the state derivative to behave as $y'(t) \sim t^{-1/2}$ as $t \to 0^+$ [3, 6]. This boundary layer singularity slightly downgrades the global interpolation accuracy of piecewise linear polynomials from $O(h^{1.5})$ to approximately $O(h^1)$. The computed EOC trends tightly mirror this theoretical constraint, confirming that the hybrid PIM-NR framework is mathematically robust, consistent, and structurally dependable under non-analytical and singular operational scenarios.

3.5 General results discussion and conclusions

In this dissertation, we have systematically designed, implemented, and validated a robust hybrid computational framework combining the Product Integration Method (PIM) with the local Newton-Raphson (NR) iterative solver to tackle weakly singular Volterra integral equations of both the first and second kinds. Through a carefully graduated series of five numerical experiments—ranging from classical linear cases to highly non-linear, non-analytical dissipative systems—the structural performance, stability, and convergence limitations of the algorithm were thoroughly exposed and analyzed [2, 5].

A comprehensive comparative synthesis of our numerical findings reveals several critical insights into the interaction between fractional singular kernels and non-linear algebraic fields:

- **Linear Regularity (Examples 1 & 2):** The framework demonstrated absolute stability in tracking linear state variables. By analytical integration of the algebraic singularity via product weights, the typical numerical instabilities near the origin $t \to 0^+$ were completely neutralized, yielding smooth error paths conforming strictly to standard Volterra thresholds [4].

- **Exact Structural Alignment (Examples 3 & 4):** In the non-linear analytical domain, the algorithm achieved remarkable milestones. Most notably, in Example 4 (non-linear Abel equation of the second kind), the maximum absolute error norm dropped to an extraordinary magnitude of $O(10^{-14})$, which effectively matches the floor of double-precision machine arithmetic. This rare accuracy is mathematically justified by the fact that the exact solution $y(t) = \sqrt{t}$ structurally neutralizes the fractional exponent of the kernel when processed through the quadratic non-linearity, reducing the local polynomial truncation error to exactly zero [9].

- **Singular Boundary Layers (Example 5):** Under non-analytical conditions where no closed-form solutions exist, the self-convergence grid study ($N_{\text{ref}} = 2000$) proved indispensable. The Experimental Order of Convergence (EOC) stabilized near 1.0. This slight reduction from the classical $O(h^{1.5})$ rate provides conclusive empirical evidence of the boundary layer singularity ($y'(t) \sim t^{-1/2}$ as $t \to 0^+$) inherent to second-kind Abel formulations, which limits global polynomial matching while maintaining rigid structural stability and monotonic root-finding behavior [3, 6].

From these rigorous validations, it can be concluded that treating the singular component analytically via PIM weight-matrices completely decouples the singularity from the step size restriction. Concurrently, utilizing localized Fréchet derivatives within the Newton-Raphson loop guarantees rapid inner convergence (typically within 3 iterations) and prevents solution bifurcation. The hybrid PIM-NR paradigm stands out as a highly reliable, mathematically sound, and computationally efficient instrument, perfectly suited for simulating complex non-linear engineering frameworks dominated by weakly singular memory kernels [7, 8].

GENERAL CONCLUSION

This dissertation has presented a rigorous and comprehensive investigation into the mathematical properties, analytical frameworks, and numerical resolutions of Abel's integral equations. By bridging the historical foundations of singular operators with modern computational quadrature schemes, we have successfully addressed the unique challenges posed by the weakly singular kernel $K(x,t) = (x-t)^{-\alpha}$ across both linear and non-linear regimes.

The theoretical insights developed in the early stages of this research underscored the dual nature of Abel equations. On one hand, their intrinsic relationship with Riemann-Liouville fractional calculus demonstrates their profound capability to capture memory mechanisms and non-local evolutionary phenomena. On the other hand, the boundary singularity inherently limits the efficacy of classical analytical and semi-analytical methodologies. While the Adomian Decomposition Method (ADM) provided elegant series expansions for certain benchmark problems, its structural reliance on explicit symbolic integrations and its steep computational cost for advanced non-linear forms revealed critical limitations. This thoroughly justified the mandatory shift toward localized, robust numerical strategies.

Consequently, the practical core of this dissertation focused on the implementation of the Product Integration Method (PIM), specifically utilizing the Product Trapezoidal Method (PTM). By factoring out the algebraic singularity to integrate it analytically, while approximating the smooth memory components via piecewise linear interpolants, the proposed scheme successfully neutralized the infinite discontinuity at the boundary. The extensive computational simulations conducted via MATLAB across five distinct illustrative frameworks fully validated the theoretical error bounds, confirming the method's rapid convergence, high accuracy, and strict numerical stability. Furthermore, the incorporation of the Newton-Raphson iterative solver for non-linear variants and the validation against a highly refined mesh reference profile demonstrated the outstanding resilience of the methodology in handling complex, non-analytical formulations.

In conclusion, the findings of this research confirm that product-based numerical integration schemes offer an exceptionally efficient, accurate, and stable paradigm for solving weakly singular Volterra integral equations. Looking forward, several promising and highly relevant avenues for future research emerge from this study:

- **Higher-order quadrature extensions:** The Product Trapezoidal framework can be extended to higher-order product formulas, such as the Product Simpson's rules, to achieve significantly accelerated rates of convergence and enhanced accuracy.

- **Systems of singular equations:** These robust computational schemes can be adapted to resolve multi-dimensional singular integral equations or coupled systems of non-linear fractional integro-differential equations, which frequently arise in advanced fluid mechanics, polymer viscoelasticity, and mathematical biology.

BIBLIOGRAPHY

[1] N. H. Abel, *Opløsning af et par opgaver ved hjælp af bestemte integraler*, Magazin for Naturvidenskaberne, Vol. 2, pp. 55–68, 1823.

[2] G. Adomian, *Solving frontier problems of physics: The decomposition method*, Kluwer Academic Publishers, 1994.

[3] K. Atkinson, *The numerical solution of integral equations of the second kind*, Cambridge University Press, 1997.

[4] R. P. Kanwal, *Linear integral equations: Theory & technique*, Birkhäuser Boston, 2nd edition, 2013.

[5] P. Linz, *Analytical and numerical methods for Volterra integral equations*, SIAM, 1985.

[6] I. Podlubny, *Fractional differential equations*, Academic Press, San Diego, 1998.

[7] M. D. Raisinghania, *Integral equations and boundary value problems*, S. Chand & Company Pvt. Ltd., New Delhi, 2013.

[8] S. G. Samko, A. A. Kilbas, and O. I. Marichev, *Fractional integrals and derivatives: Theory and applications*, Gordon and Breach Science Publishers, 1993.

[9] A. M. Wazwaz, *Linear and nonlinear integral equations: Methods and applications*, Springer Science & Business Media, 2011.

•Abstract:

This research presents a robust computational framework for the numerical solution of Abel integral equations through the implementation of advanced numerical methodologies using MATLAB. The study provides an in-depth investigation into the precise treatment of Volterra-type integral equations of the first kind, with a specific focus on the Abel integral equation, which finds extensive applications across various scientific and engineering domains.

Keywords: Abel Integral Equations, Singular Integral Equations, Numerical Methods, MATLAB Implementation, Computational Mathematics, Volterra Equations.

•Résumé :

Cette recherche présente un cadre computationnel robuste pour la résolution numérique des équations intégrales d'Abel à travers la mise en œuvre de méthodologies numériques avancées sous MATLAB. L'étude propose une investigation approfondie du traitement précis des équations intégrales de type Volterra de première espèce, en mettant particulièrement l'accent sur l'équation intégrale d'Abel, qui trouve de vastes applications dans divers domaines scientifiques et de l'ingénierie.

Mots-clés : Équations intégrales d'Abel, Équations intégrales singulières, Méthodes numériques, Implémentation MATLAB, Mathématiques de calcul, Équations de Volterra.

•ملخص:

يقدم هذا البحث إطاراً حاسوبياً قوياً للحل العددي لمعادلات أبلْ التكاملية من خلال تطبيق منهجيات عددية متقدمة باستخدام برنامج ماتلاب. تقدمْ الدراسة تحليلاً وتدقيقاً عميقاً في المعالجة الدقيقة لمعادلات فولتيرْ التكاملية من النوع الأول، مع تركيز خاص على معادلة أبلْ التكاملية، والتي تجد تطبيقات واسعة النطاق في مختلف المجالات العلمية والهندسية.

الكلمات المفتاحية: معادلات أبل التكاملية، المعادلات التكاملية المفردة، الطرق العددية، تطبيق ماتلاب، الرياضيات الحاسوبية، معادلات فولتير.